

Robust face and facial feature localization using the dual skin model

Wei Li*

Computer School, China West Normal University, Shida Rd. 1, Nanchong, Sichuan, China

Received 1 March 2014, www.cmmt.lv

Abstract

A fast and adaptive face and facial feature localization algorithm for colour images with sophisticated background is present. In this algorithm, a self-adaptive pre-processing method was provided to depress the colour bias and the high light. Then the CbgCbr-YIQ dual skin model was proposed to acquire the integrated skin similarity for improving the quality of skin segmentation and extraction. After the morphological post-processing, by using the Adaboost classifier and the information of spatial position, the facial feature positioning was fast realized finally. Experimental results showed the robustness and good performance of the proposed algorithm.

Keywords: pre-processing, dual skin model, facial feature localization, face recognition, Adaboost

1 Introduction

In research, fields such as image understand and computer vision, as an important stage or a key problem in face recognition, the face and facial feature localization often has received significant attention. Variety of methods were proposed to solve the face detection problem, such as the method based on template matching [1], method based on classifier [2-5], method based on colour and space features [6,7]. For the first method, it may be spent too much time on the calculation of matching. For the second method, the accuracy and stability of detection is greatly affected by the trained classifier and chose samples. For the third method, the accuracy of facial feature localization depends on the built skin model and the results of skin segmentation. The algorithm in this paper combined the advantage of classifier and advantages of colour and space features. First, an adaptive pre-processing method was proposed to improve the quality of input image. Second, a new CbgCbr-YIQ dual skin model was built to acquire the integrated similarity for skin segmentation and extraction. Then the face candidates came from the hole-filled skin-extracted image was got by morphological post-processing. Finally the face candidates based on the dual skin model were regarded as the testing objects of Adaboost classifier, and the spatial information of facial features were jointly used to localize the facial features for the face image.

2 Algorithm flow

As shown in Figure 1, the algorithm is consisted of five stages:

1. Pre-processing: use pre-processing to depress the colour excursion and high light for improving the quality of

original image (Figure 1a). Accordingly the pre-processed image can be acquired (Figure 1b).

2. Building the dual skin model and acquiring integrated similarity: the CbgCbr-YIQ dual skin model consisted of the CbgCbr ellipse model and the adaptive YIQ model. It aimed to combine features of two models. Figures 1c and 1d showed the corresponding skin-similarity images based on CbgCbr and YIQ models. In this stage, the integrated similarity image can be acquired (Figure 1e) based on the CbgCbr-YIQ dual skin model.

3. Skin segmentation and extraction: based on integrated similarity, skin-segmented and skin-extracted images can be acquired by binary segmentation and extraction, as shown in Figures 1f and 1g.

4. Post-processing: use morphological technology contained the noise reduction and hole filling to realize the post-processing and prepare for the subsequence localization. With the noise reduction technology in post-processing, the denoised skin-segmented image and denoised skin-extracted image can be acquired (Figures 1h and 1i). With the hole filling technology, the hole-filled skin-segmented image and hole-filled skin-extracted image can be acquired (Figures 1j and 1k). The denoised skin-segmented or skin-extracted image decreased the noise disturbance but preserve the facial features. The hole-fill skin-segmented image or skin-extracted image contained the face candidates' targets.

5. Positioning face and facial features: Use Adaboost classifier to detect face targets in face candidates' targets. Accordingly, the hole-filled face-segmented image and hole-filled face-extracted image can be acquired (Figures 1m and 1n). Besides the denoised face-segmented image and denoised face-extracted image can be acquired (Figures 1o and 1p). By difference and combined using the

*Corresponding author e-mail: nos036@163.com

spatial information of facial features, the facial features can be localized (Figures 1p, 1q and 1r).

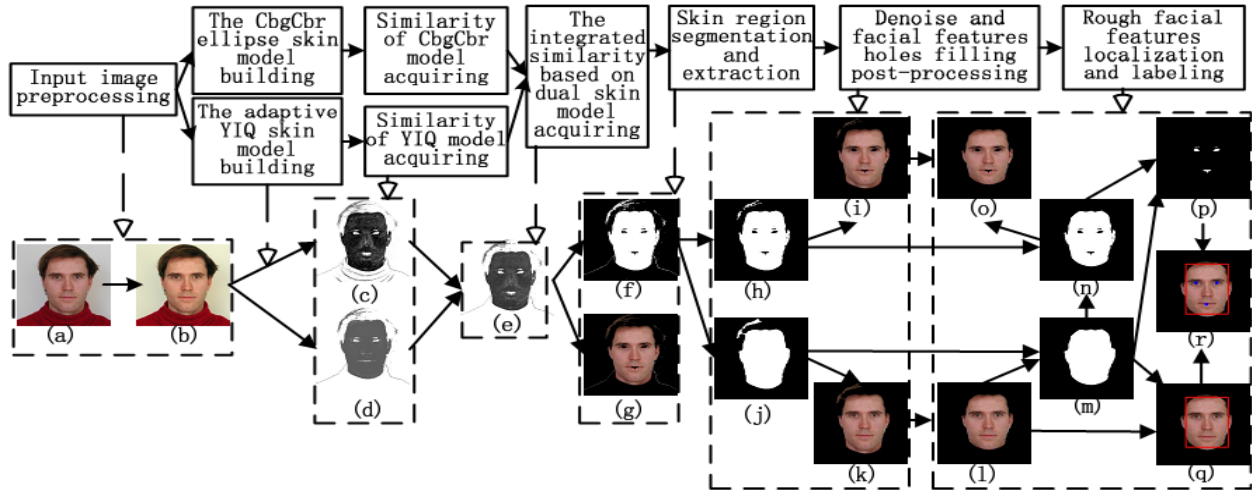


FIGURE 1 The algorithm flow: a) input image, b) pre-processed image, c) skin-probability image of CbgCbr ellipse model, d) skin-probability image of YIQ model, e) integrated probability image of dual skin model, f) skin-segmented image based on dual skin model, g) skin-extracted image based on dual skin model, h) denoised skin-segmented image, i) hole-filled skin-segmented image, j) hole-filled skin-extracted image, k) hole-filled skin-extracted image, l) hole-filled face-extracted image, m) hole-filled face-extracted image, n) denoised face-extracted image, o) denoised face-extracted image, p) feature image, q) face-localized image, r) face and facial features localized image

3 Pre-processing

The quality of colour input image is often affected greatly by input device and environment. The problems of colour excursion and high light are often caused by sophisticated background and variant light conditions. For improving the quality of colour input image and helping to the subsequent operations (e.g. skin segmentation and extraction), the proposed pre-processing in this paper aimed to adjust the colour and brightness adaptively to depress the colour excursion and the high light. The main steps of pre-processing are as follows:

Step 1: Accumulate separately $R_{i,j}$, $G_{i,j}$, $B_{i,j}$ and $Y_{i,j}$ components of every pixel to calculate their average values: aR , aG , aB and aY using Equation (1):

$$Y_{i,j} = 0.299 \times R_{i,j} + 0.578 \times G_{i,j} + 0.114 \times B_{i,j},$$

$$\left\{ \begin{array}{l} aR = \frac{\sum_{j=0}^H \sum_{i=0}^W R_{i,j}}{(H \times W)}, \quad aG = \frac{\sum_{j=0}^H \sum_{i=0}^W G_{i,j}}{(H \times W)}, \\ aB = \frac{\sum_{j=0}^H \sum_{i=0}^W B_{i,j}}{(H \times W)}, \quad aY = \frac{\sum_{j=0}^H \sum_{i=0}^W Y_{i,j}}{(H \times W)} \end{array} \right. , \quad (1)$$

where, H and W are the height and the width of the input image, i and j are a point's abscissa and ordinate of the input image.

Step 2: Use aR , aG , aB and aY in Equation (2) to calculate the adjustment coefficients: cR , cG and cB .

$$cR = \frac{aY}{aR}, cG = \frac{aY}{aG}, cB = \frac{aY}{aB}. \quad (2)$$

Step 3: Using Equation (3), use $R_{i,j}$, $G_{i,j}$, $B_{i,j}$ and $Y_{i,j}$ components of every pixel to calculate light adjustment coefficients: $lR_{i,j}$, $lG_{i,j}$, $lB_{i,j}$.

$$\left\{ \begin{array}{l} lR_{i,j} = \left[a \tan \left(\frac{R_{i,j}}{Y_{i,j}} \right) + a \tan \left(\frac{R_{i,j} + G_{i,j} + B_{i,j}}{R_{i,j} \times 3} \right) \right] \times 0.5 \\ lG_{i,j} = \left[a \tan \left(\frac{G_{i,j}}{Y_{i,j}} \right) + a \tan \left(\frac{R_{i,j} + G_{i,j} + B_{i,j}}{G_{i,j} \times 3} \right) \right] \times 0.5 \\ lB_{i,j} = \left[a \tan \left(\frac{B_{i,j}}{Y_{i,j}} \right) + a \tan \left(\frac{R_{i,j} + G_{i,j} + B_{i,j}}{B_{i,j} \times 3} \right) \right] \times 0.5 \end{array} \right. . \quad (3)$$

Step 4: By Equations (4) and (5), use the colour adjustment coefficients and the light adjustment coefficients to adjust the $R_{i,j}$, $G_{i,j}$, $B_{i,j}$ components and acquire the adjusted $R'_{i,j}$, $G'_{i,j}$, $B'_{i,j}$ components:

$$\left\{ \begin{array}{l} R'_{i,j} = R_{i,j} \times cR \times lR_{i,j} \\ G'_{i,j} = G_{i,j} \times cG \times lG_{i,j} \\ B'_{i,j} = B_{i,j} \times cB \times lB_{i,j} \end{array} \right. , \quad (4)$$

$$\left\{ \begin{array}{l} R'_{i,j} = 255 \text{ if } (R'_{i,j} > 255) \\ G'_{i,j} = 255 \text{ if } (G'_{i,j} > 255) \\ B'_{i,j} = 255 \text{ if } (B'_{i,j} > 255) \end{array} \right. . \quad (5)$$

Step 5: Normalize separately the $R'_{i,j}$, $G'_{i,j}$, $B'_{i,j}$ components of input image to the range [0 255].

Figure 2 shows an example of pre-processing. Comparing Figures 2a and 2b, Figures 2g and 2h, Figures 2i and 2j, note that the colour bias and the high light were depressed partly. Comparing Figures 2c and 2d, Figures 2e

and 2f, it's easy to find that, with this pre-processing, the typical segmentation method (based on CbCr Gaussian skin model or CbCr ellipse skin model) segmented fewer non-skin pixels and more real skin pixels, the owe or excessive segmentation was decreased.

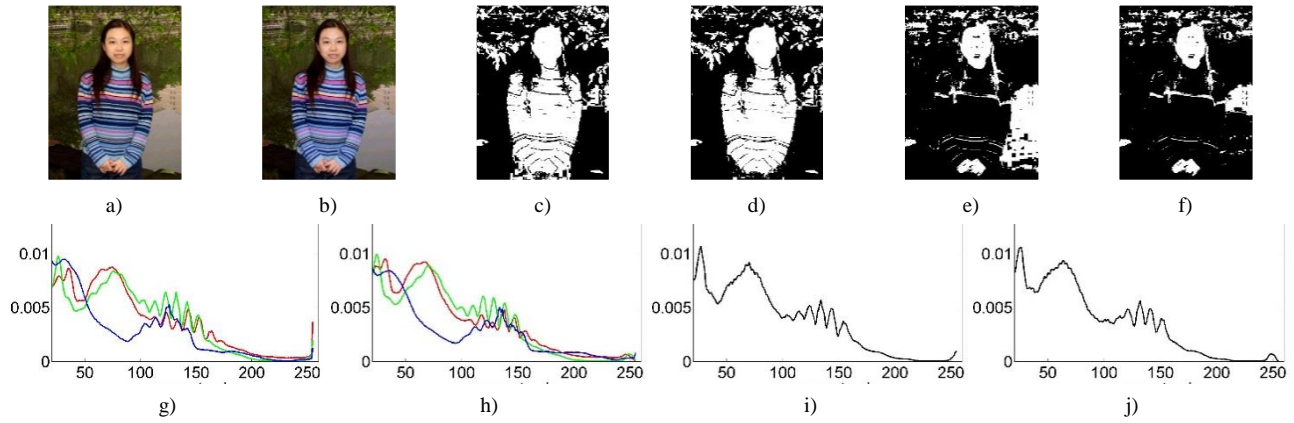


FIGURE 2 Image pre-processing: a) input image, b) pre-processed image, c) skin-segmented image of a) based on CbCr Gaussian model, d) skin-segmented image of b) based on CbCr Gaussian model, e) skin-segmented image of a) based on CbCr ellipse model, f) skin-segmented image of b) based on CbCr ellipse model, g) probability density distribution of R,G,B components of a), h) probability density distribution of R,G,B components of b), i) probability density distribution of Y component of a), j) probability density distribution of Y component of b)

4 Skin segmentation

Skin colour space and skin model used by colour image is very useful and important for skin segmentation and skin extraction. Used colour space commonly include RGB, YCbCr, YIQ, HSV, etc., the basic colour space is RGB, while the other colour spaces are transformed from RGB. The typical skin models include Gaussian model [1, 8], ellipse model [6], and the other models [9]. The single skin model may lose some information of skin colour and facial features in input image. Especially for image with colour excursion and high light, the insufficient and over segmentation based on a single skin model often occurred. The model's ability of skin description should be enhanced to improve accuracy of skin segmentation, and application scope of skin model still need to enlarge. To solve these problems, this paper built a CbgCbr-YIQ dual skin model to acquire the skin similarity, which reflected the distribution of skin colour better and get better segmentation results than a single skin model.

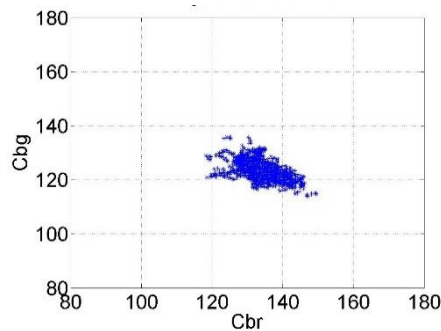


FIGURE 3 Skin color cluster in CbgCbr 2D color space

4.1 THE CBGCBR SKIN MODEL

The CbgCbr skin model originated from the CbgCbr 2D colour space and the average thought. As mentioned above, the pre-processed image (Figure 1b) can be acquired by pre-processing the original input image (Figure 1a). The original input image mainly came from the MIT single face test set [10] and self-built multi-face test set. This paper regarded the skin samples of pre-processed images as statistic sources. According to statistics, skin cluster analysis of skin samples showed that, the distribution of skin colour cluster presented a 2D ellipse in CbgCbr 2D colour space (Figure 3). So the CbgCbr ellipse skin model was built on the basis of skin cluster (Equations (6)-(9)). Based on CbgCbr ellipse skin model, the skin similarity can be calculated (Equation (9)), and skin-similarity image can be acquired (Equation (10) and Figure 1(c)). The steps of similarity calculation based on CbgCbr model are as follows:

Step 1: Acquire $Y'_{i,j}$, $Cr_{i,j}$, $Cg_{i,j}$, $Cb_{i,j}$ components of pre-processed image using Equations (6)-(7).

$$Y'_{i,j} = 0.299 \times R'_{i,j} + 0.578 \times G'_{i,j} + 0.114 \times B'_{i,j}, \quad (6)$$

$$\begin{bmatrix} Cr_{i,j} \\ Cg_{i,j} \\ Cb_{i,j} \end{bmatrix} = \begin{bmatrix} 128 \\ 128 \\ 128 \end{bmatrix} + \begin{bmatrix} 0.713 & 0 & 0 \\ 0 & 0.587 & 0 \\ 0 & 0 & 0.564 \end{bmatrix} \begin{bmatrix} R'_{i,j} - Y'_{i,j} \\ G'_{i,j} - Y'_{i,j} \\ B'_{i,j} - Y'_{i,j} \end{bmatrix}, \quad (7)$$

Step 2: Use Equation (8) to calculate three average components: $Cbr_{i,j}$, $Cgr_{i,j}$, $Cbg_{i,j}$.

$$Cbr_{i,j} = \frac{Cb_{i,j} + Cr_{i,j}}{2}, Cgr_{i,j} = \frac{Cg_{i,j} + Cr_{i,j}}{2}, \quad (8)$$

$$Cbg_{i,j} = \frac{Cb_{i,j} + Cg_{i,j}}{2}$$

Step 3: Build the CbgCbr ellipse skin model. Based on this model, calculate the similarity by Equation (9). Acquire the similarity image by Equation (10) and the skin-segmented image by Equation (11).

$$S_{i,j} = \frac{(Cbr_{i,j} - 135)^2}{(12)^2} + \frac{(Cbg_{i,j} - 115)^2}{(10)^2}, \quad (9)$$

$$P_{i,j} = \begin{cases} S_{i,j} \times 255 & \text{if } (S_{i,j} \leq 1) \\ 255 & \text{else} \end{cases} m, \quad (10)$$

$$F_{i,j} = \begin{cases} 255 & \text{if } (S_{i,j} \leq 1) \\ 0 & \text{else} \end{cases} m, \quad (11)$$

where $P_{i,j}$ and $F_{i,j}$ are the pixel's value of skin-similarity image and the pixel's value of skin-segmented image based on CbgCbr skin model.

4.2 THE ADAPTIVE YIQ SKIN MODEL

Lots of experiments and existing research demonstrated that the appearance of skin colour shows some degree clustering characteristic in YIQ colour space. The YIQ skin model originated from the clustering distribution of skin colour in the YIQ 2D colour space and the difference thought between I and Q components. This paper built an adaptive skin model in YIQ colour space to calculate skin similarity (Equation (13)) of pre-processed image, and correspondingly to acquire the similarity image (Equation (14) and Figure 1d). The steps of skin similarity calculation based on YIQ skin model are as follows:

Step 1: Acquire $Y'_{i,j}$, $I_{i,j}$ and $Q_{i,j}$ components of pre-processed image using Equation (12):

$$\begin{bmatrix} Y'_{i,j} \\ I_{i,j} \\ Q_{i,j} \end{bmatrix} = \begin{bmatrix} 0.299 & 0.587 & 0.114 \\ 0.596 & -0.274 & -0.322 \\ 0.212 & -0.523 & -0.311 \end{bmatrix} \begin{bmatrix} B'_{i,j} \\ G'_{i,j} \\ R'_{i,j} \end{bmatrix}, \quad (12)$$

Step 2: Build the adaptive YIQ skin model. Based on this model, calculate the similarity by Equation (13). Acquire the similarity image by Equation (14) and segmented image by Equation (15).

$$\begin{cases} t'_{i,j} = \frac{(I_{i,j})^2}{(Y'_{i,j})^2} + \frac{(Q_{i,j})^2}{(Y'_{i,j})^2}, \\ t''_{i,j} = \frac{\sqrt{(I_{i,j} - Q_{i,j})^2}}{Y'_{i,j}}, \quad S'_{i,j} = \frac{t'_{i,j}}{t''_{i,j}} \end{cases}, \quad (13)$$

$$P'_{i,j} = \begin{cases} S'_{i,j} \times 255 & \text{if } (S'_{i,j} \leq 1 \text{ and } I_{i,j} > 20) \\ 255 & \text{else} \end{cases}, \quad (14)$$

$$F'_{i,j} = \begin{cases} 255 & \text{if } (S'_{i,j} \leq 1 \text{ and } I_{i,j} > 20) \\ 0 & \text{else} \end{cases}, \quad (15)$$

where, the $P'_{i,j}$ and $F'_{i,j}$ are the pixel's value of skin similarity image and the pixel's value of skin-segmented image based on YIQ skin model.

4.3 THE INTEGRATED SIMILARITY BASED ON THE DUAL SKIN MODEL

The calculation of the integrated similarity is to get the average value of two kinds of similarities based on the CbgCbr model and the YIQ adaptive model. It can combine advantages of two skin models, and make the integrated skin similarity had better accuracy, adaptability, and ability of skin description, especially in the case of different races, sophisticated background and variant light. So after acquiring two kinds of similarities ($S_{i,j}$ and $S'_{i,j}$), the integrated similarity $S''_{i,j}$ based on the dual skin model can be acquired using Equation (16). So the integrated similarity image is an image that fused two similarity images conditionally (Equation (17) and Figure 1e).

$$S''_{i,j} = \frac{(S'_{i,j} + S_{i,j})}{2}, \quad (16)$$

$$P''_{i,j} = \begin{cases} S''_{i,j} \times 255 & \text{if } (S''_{i,j} < 1 \text{ and } S_{i,j} < 1 \text{ and } S'_{i,j} < 1) \\ 255 & \text{else} \end{cases}, \quad (17)$$

$$F''_{i,j} = \begin{cases} 255 & \text{if } (S''_{i,j} < 1 \text{ and } S_{i,j} < 1 \text{ and } S'_{i,j} < 1) \\ 0 & \text{else} \end{cases}, \quad (18)$$

$$\begin{cases} R''_{i,j} = R'_{i,j}, G''_{i,j} = G'_{i,j}, B''_{i,j} = B'_{i,j} \\ R''_{i,j} = G''_{i,j} = B''_{i,j} = 0 \text{ if } (S''_{i,j} \geq 1 \text{ or } S_{i,j} \geq 1 \text{ or } S'_{i,j} \geq 1) \end{cases}. \quad (19)$$

After acquiring the integrated skin similarity, by judging and binary segmenting non-white pixels of integrated similarity image (Equation (18)) and reserving corresponding region of pre-processed image (Equation (19)), skin-segmented image and skin-extracted image can be acquired (Figures 1f and 1g).

Figure 4 shows the examples of skin segmentation based on several skin models, including CbCr Gaussian model, CbCr ellipse model, CbgCbr ellipse model, YIQ adaptive model, CbgCbr-YIQ dual model. These models were built for the pre-processed image (Figure 4(a)). Comparing Figures 4d and 4e, or Figures 4j and 4k, note that the skin regions approximately have the same positions in two images, but the non-skin regions or noise regions are different partly. Based on these characteristics above, the integrated similarity image (Figure 4f) fused two similarity images by averaging and logical conditions

(Equations (16) and (17)) to preserve the real skin regions and remove the non-skin regions. From Figures 4j, 4k and 4l, it's easy to find that the skin-segmented image based on dual skin model had fewer non-skin pixels and preserved more real skin pixels, the owe segmentation or excessive

segmentation was decreased. Comparing Figure 4h, 4i and 4l, it is obvious that relative to the CbCr Gaussian model and CbCr ellipse model, the segmented image based on dual skin model had less error segmentation.

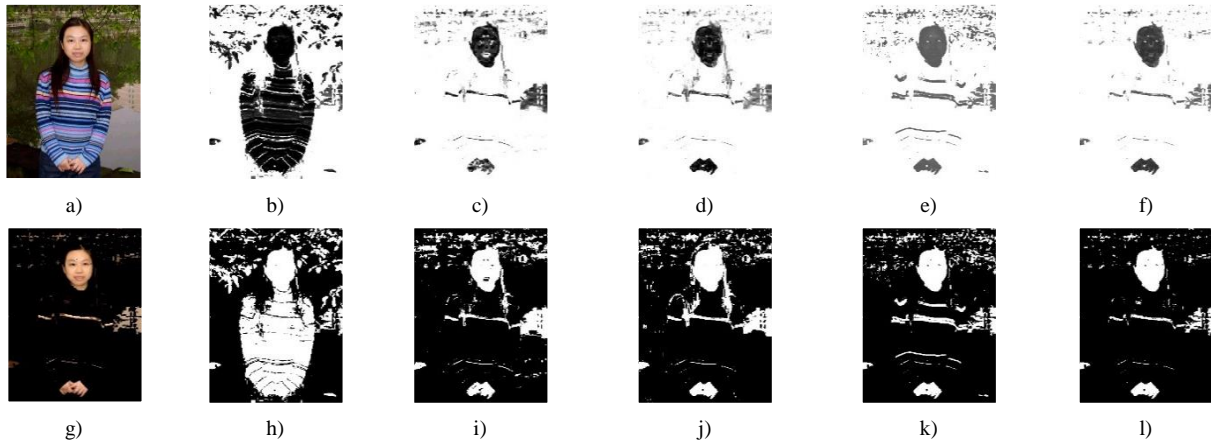


FIGURE 4 Skin segmentation and extraction: a) pre-processed image, b) similarity image of a) based on CbCr Gaussian model, c) similarity image of a) based on CbCr ellipse model, d) similarity image of a) based on CbgCbr ellipse model, e) similarity image of a) based on YIQ model, f) similarity image of a) based on CbgCbr-YIQ dual model, g) skin-extracted image based on f), h) skin-segmented image based on b), i) skin-segmented image based on c), j) skin-segmented image based on d), k) skin-segmented image based on e), l) skin-segmented image based on f)

5 Post-processing and localization

As stated above, the skin-segmented image and the skin-extracted image can be acquired based on the dual skin model. The skin-segmented image (Figure 4l) and the skin-extracted image both contained all the possible skin regions, including the real face objects, the non-face skin objects (such as hands, foots, legs, etc.), non-skin objects (skin-similar backgrounds), and some noise. In order to search the face regions and localize the facial features roughly as soon as possible, the morphological post-processing, the Adaboost classifier [24], the gradient [11] and difference technology were used in this part jointly. To depress or remove the noise interference, and to acquire

the face candidates, the post-processing adopted the morphological close operation and open operation, using the 3×3 template. With the close operation, the denoised skin-segmented image and the corresponding denoised skin-extracted image can be acquired (Figure 5b and 5h), which preserved the facial feature holes (e.g. eyes and mouth). With the open operation, the hole-filled skin-segmented image and the corresponding hole-filled skin-extracted image can be acquired (Figure 5c and 5i), which contained the all the face candidates. Moreover, the face candidates in hole-filled skin-extracted image (Figure 5i) are about to be detected or classified by trained Adaboost classifier.

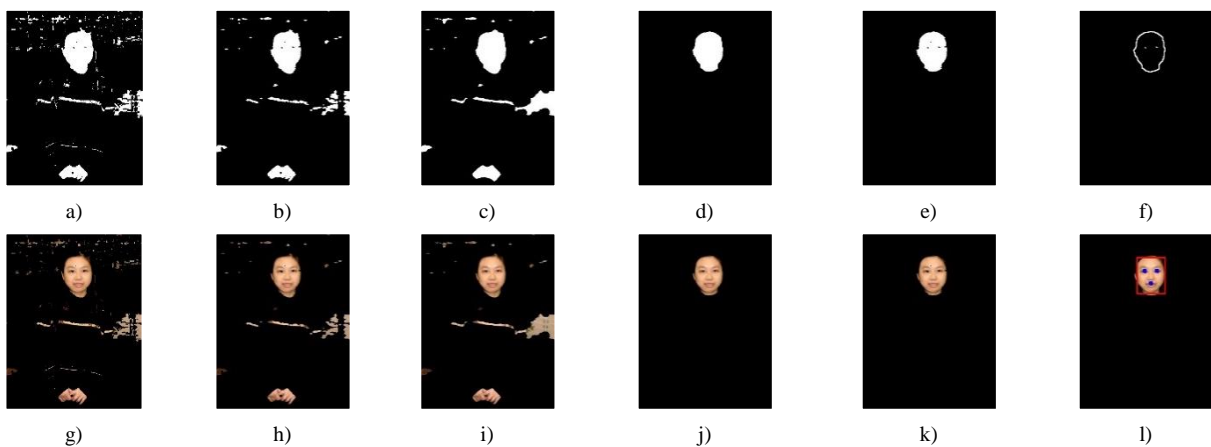


FIGURE 5 Post-processing and facial features localization: a) skin-segmented image based on CbgCbr-YIQ dual skin model, b) denoised skin-segmented image, c) hole-filled skin-segmented image, d) hole-filled face-segmented image, e) denoised face-segmented image (with facial feature holes), f) facial feature image g) skin-extracted image based on CbgCbr-YIQ dual skin model, h) denoised skin-extracted image, i) hole-filled skin-extracted image, j) hole-filled face-extracted image, k) denoised face-extracted image (with facial feature holes), l) face and facial feature localized image

As the hole-filled skin-segmented image and hole-filled skin-extracted image contained all the face candidates, some of which is the possible non-face objects. For removing the non-face regions, and acquiring the real face regions, the Adaboost classifier was used. There was a problem that how to narrow the range of searching or scanning. To solve this problem, the face candidates in the hole-filled skin-extracted image (Figure 5(i)) were regarded as the being detected or classified targets by Adaboost classifier, which was trained by face samples in the training set. Generally, the used object detected by classifier is a whole image, which spent too much time to scan or search all the pixels in the whole image. This classifier scanned the face candidate regions instead of all the pixels in the whole image. After judging and classifying, it discarded the non-face objects and preserved the face objects in hole-filled skin-extracted image (Figure 5(i)). So the extracted face target in the hole-filled face-extracted image can be acquired, as shown in Figure 5(j). This way not only can improve the speed of scanning and save the time of searching, but also increase the accuracy of detection. With Adaboost classifier, face regions in hole-filled face-extracted image can be got (Figure 5j), and the corresponding face-segmented image (Figure 5d) can be acquired. Moreover, the denoised face-segmented image with facial feature holes (Figure 5e) and corresponding denoised face-extracted image with holes (Figure 5k) also can be acquired. By comparison, it is thus clear that Figures 5d and 5e is different in facial feature regions (eyes and mouth regions). Using the difference technology and Gradient limitation, the facial feature image can be acquired (Figure 5f), and then facial feature localization can be realized (Figure 5l).

6 Experiment

The proposed method was tested on MIT face test set [10] and a self-built test set to evaluate its performance. The MIT face test set contains 50 images of 10 individuals, with different colour bias, variant light and poses. The self-built test set contains 100 images with 585 faces, gathered with different poses and expressions, variant light and sophisticated background. Each image can be rescale automatically to a standard size (150×150 pixels). The test condition is: P4, 2GHz CPU, 2G memory, and VC6. Based on two groups of test sets (single-face and multi-face), the average time in each stage of this algorithm was shown in Figure 6, where the average time on single-face test set was slightly higher than those on multi-face test set. Table 1 listed comparison of localization rates of proposed algorithm and the other algorithms. It is easy to find that the localization rate of this algorithm is higher than that of others, but the speed is fast. There are five examples shown in Figure 7, which contained the images with variant poses, variant light, sophisticated background, multiple faces.

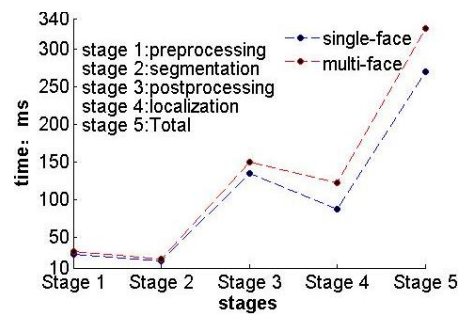


FIGURE 6 Average time in each stage

TABLE 1 Comparison of localization rate (Image Size:150×150)

No	Algorithm	Localization Rate	Test samples (No. of images/faces)
1	Algorithm based on template matching	80.8%	30 colour images (150)
2	Algorithm based on Gaussian model	84.1%	25 colour images (125)
3	Algorithm based on ellipse model	82.9%	25 colour images (125)
4	Algorithm based on Gaussian model+template matching [1]	97.2%	25 colour images (150)
5	Algorithm based on Bayes [3]	95.6%	20 grayscale images (130)
6	Algorithm based on Adaboost [4]	85.7%	30 colour images (150)
7	Algorithm based on Neural Network [5]	84.5%	25 grayscale images (125)
8	Algorithm based on lighting compensation+ ellipse mode [6]	92.5%	35 colour images (175)
9	Algorithm based on Gaussian model+PCA [12]	93.3%	25 colour images (150)
10	Proposed Algorithm in This Paper (the dual model+Adaboost)	98.3%	150 colour images (635)

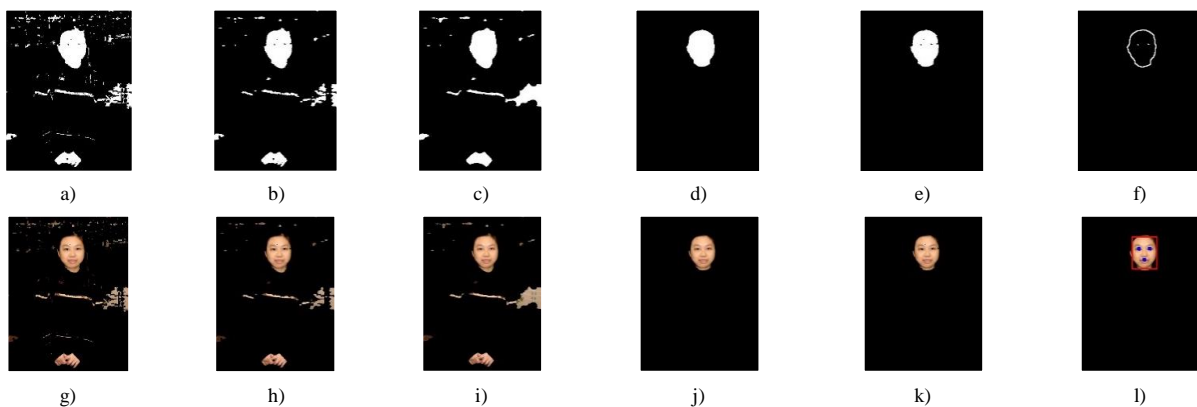


FIGURE 7 Examples of facial feature localization: a) d) g) j) m) p) colour input images, b) e) h) k) n) q) facial feature localized images (background removed), c) f) l) o) r) facial feature localized images

7 Conclusions

A Face and facial feature localization algorithm based on CbgCbr-YIQ dual skin model was presented in this paper. To improve the accuracy of skin segmentation, as well as the speed of the face and facial feature localization, the proposed algorithm contains pre-processing, building the dual skin model, skin segmentation and extraction, post-processing, face and facial feature positioning. The pre-processing depressed colour excursion and high light partly. Then the built dual skin model had better ability of skin description, adaptability and robustness than the single skin model. The skin segmentation and extraction based on dual skin model obtained fewer non-skin objects and more skin objects. The morphological post-processing removed noise fast, provided face candidates for Adaboost

classifier and helped to decrease the range of scanning greatly. The face and facial feature positioning was realized by jointly using the classifier, the difference and gradient limitation technologies. The experimental results demonstrated that this algorithm had robustness and good performance for colour face image with sophisticated background, variant light, multiple poses and expressions.

Acknowledgements

This work was supported in part by Sichuan Provincial Department of Science and Technology Supporting Project (No. 2012GZ0020), the Scientific Research Foundation of the Education Department of Sichuan Province of China (No. 13ZB0012).

References

- [1] Wang Z, Li S 2011 *Information Technology Journal* **10**(12) 2308-14
- [2] Guo J M, Lin C C, Wu M F, Chang C H, Lee H 2011 *IEEE Signal Proc Let* **18**(8) 447-50
- [3] Wang Y, Wu Y 2010 *Pattern Recognition* **43**(3) 1008-15
- [4] Yang M, Crenshaw J, Augustine B 2010 *Computer Visual and Image Understanding* **114**(11) 1116-25
- [5] Wang Z, Li T 2008 A Face Detection System Based Skin Color and Neural Network *Proceedings of 2008 International Conference on Computer Science and Software Engineering* **1** 961-4
- [6] Hsu R L, Mottaleb M A, Jain A K 2002 *IEEE Transactions on Patter Anal Mach Intell.* **24**(5) 696-706
- [7] Ibrahim N B, Selim M M, Zayed H H 2012 A dynamic skin detector based on face skin tone color *Proc of 2012 8th Int Conf on Informatics and Systems MM-1-MM-5*
- [8] Tan W R, Chan C S, Yogarajah P, Condell J 2012 *IEEE Transactopm on Industrial Informatics* **8**(1) 138-47
- [9] Chu H, Xie Z, Xu X, Zhou L, Liu Q 2011 Inspection and Recognition of Generalized Surface Defect for Precise Optical Elements *Information Technology Journal* **10**(7) 1395-401
- [10] *CBCL Face Recognition Database* <http://cbcl.mit.edu/software-datasets/heisele/facerecognition-database.html> 15 Nov 2013
- [11] Niu Z H, Shan S G, Chen X L 2009 *IEEE Signal Processing Letters* **16**(10) 897-900
- [12] Shih F Y, Cheng S X, Chuang C F, Wang P S P 2008 *Patt Recog Artif Intell* **22**(3) 515-34

Author



Wei Li, born in February, 1982, Sichuan, China

Current position, grades: lecturer Computer school, China West Normal University.

University studies: BSc degree in computer science and technology from China West Normal University (P.R.C.) in 2004. MSc degree in communication engineering from the Chongqing University (P.R.C.) in 2007.

Scientific interest: pattern recognition, signal processing, image processing, and embedded system.

Publications: 8 papers.